SAND2019-14744C

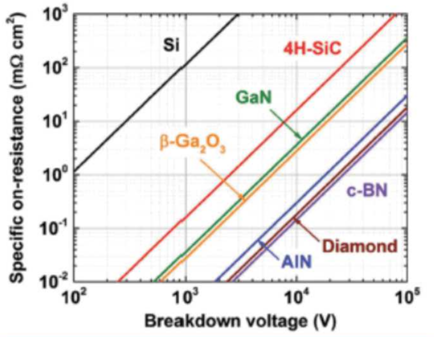

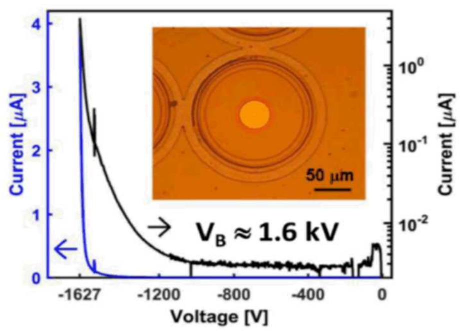

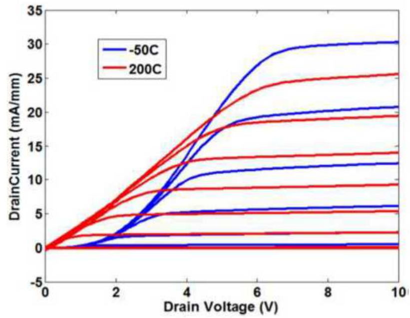

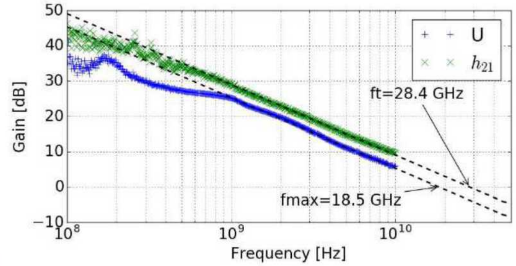

Ultra-Wide-Bandgap Aluminum Gallium Nitride for High-Performance Power-Switching and Radio-Frequency Devices

Workshop on Innovative Nanoscale Devices and Systems (WINDS)
Kohala Coast, Hawaii, USA
December 4, 2019

Robert Kaplar, Andrew Armstrong, Albert Baca, Brianna Klein, Erica Douglas, Shahed Reza, Andrew Allerman, Mary Crawford, Jeramy Dickerson, Andrew Binder, Jack Flicker, Jason Neely, and Oleksiy Slobodyan

Sandia National Laboratories, Albuquerque, NM

Sandia National Laboratories is a multi-program laboratory managed and operated by National Technology & Engineering Solutions of Sandia, LLC (NTESS), a wholly owned subsidiary of Honeywell Corporation, for the U.S. Department of Energy's National Nuclear Security Administration under contract DE-NA0003525.

Outline

- Motivation for UWBG Semiconductors
- Vertical AlGaN PiN Diodes for Power Switching
- Lateral AlGaN HEMTs for Power Switching
- Lateral AlGaN HEMTS for RF Applications

Outline

- Motivation for UWBG Semiconductors
- Vertical AlGaN PiN Diodes
- Lateral AlGaN HEMTs for Power Switching
- Lateral AlGaN HEMTS for RF Applications

Critical Electric Field for Avalanche Breakdown

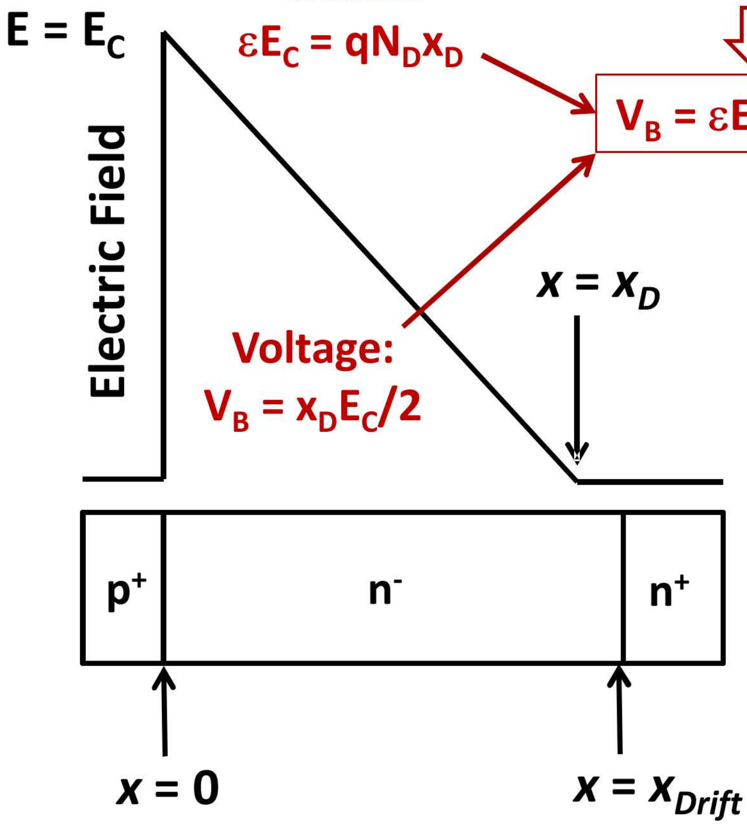

Gauss: $\varepsilon E_C = qN_D x_D$

Voltage: $V_B = x_D E_C/2$

$V_B = \varepsilon E_C^2/2qN_D$

Resistance: $R_{on,sp} = W_D/q\mu_n N_D$

$V_B^2/R_{on,sp} = \varepsilon \mu_n E_C^3/4$

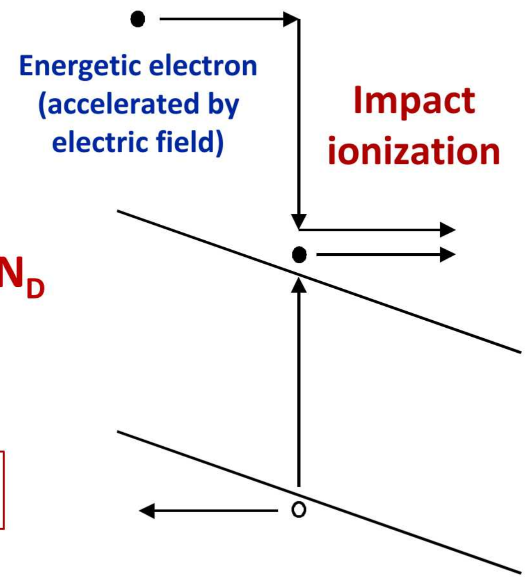

$$M_n = \frac{exp\left[\int_0^{x_D}\left(\alpha_n(x) - \alpha_p(x)\right)dx\right]}{1 - \int_0^{x_D}\alpha_p(x)\cdot exp\left[\int_x^{x_D}\left(\alpha_n(x') - \alpha_p(x')\right)dx'\right]dx}$$

Avalanche occurs when denominator approaches zero

The critical field is defined as the maximum electric field that leads to avalanche breakdown in a 1D analytical model

Critical Electric Field Scales with Bandgap and Determines Unipolar FOM

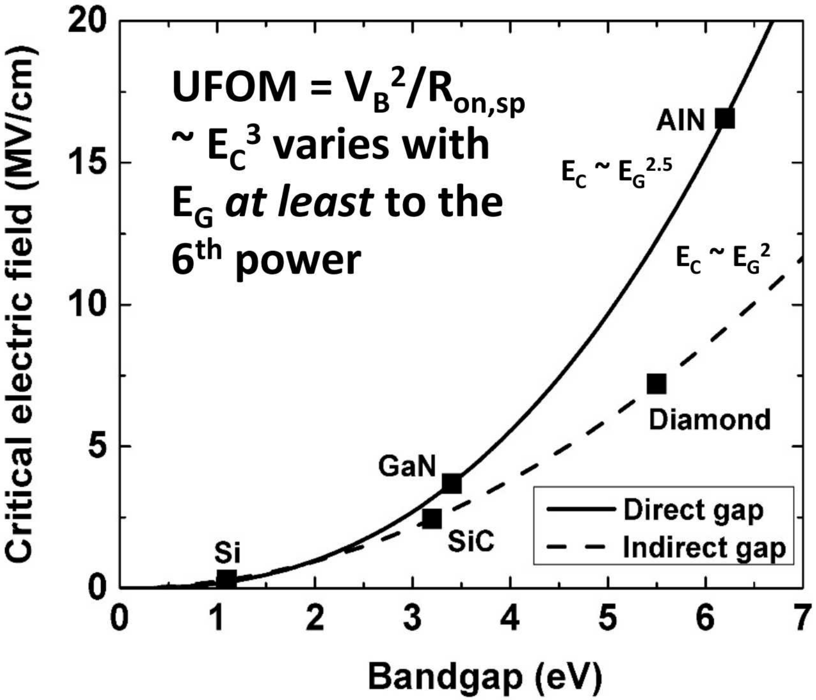

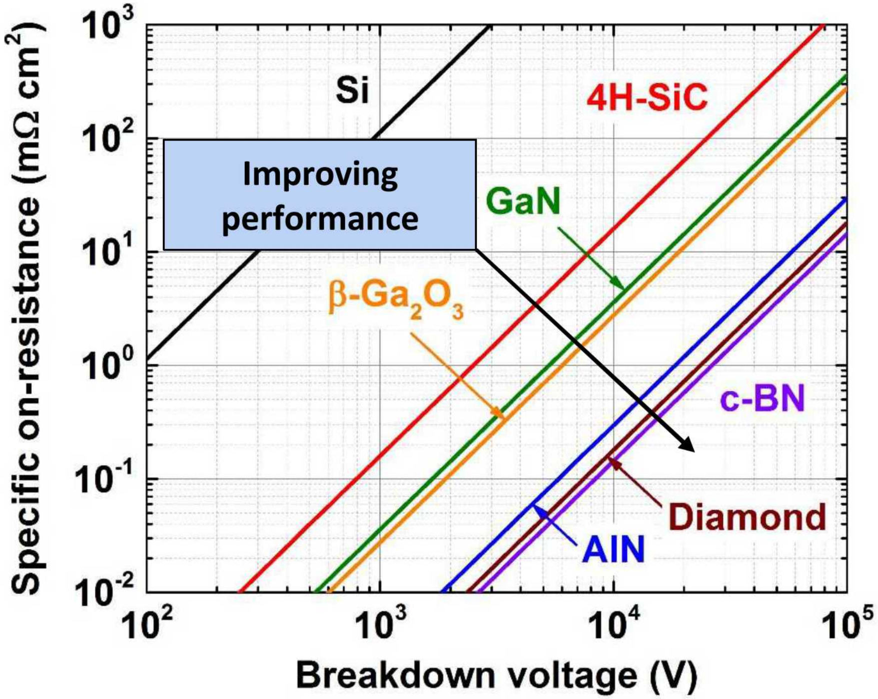

Unipolar FOM = $V_B^2/R_{on,sp} = \varepsilon\mu_n E_C^3/4$

Hudgins et al., *IEEE Trans. Pwr. Elec.* 18, 907 (2003); J. Y. Tsao et al., *Adv. Elec. Mat. Adv. Elec. Mat.* 4, 1600501 (2018)

Origin of 2.0 and 2.5 Power-Law Fits for Indirect- and Direct-Gap Semiconductors

- **Empirical fits used to predict the capabilities of emerging materials: $\mathcal{E}_{crit} \sim E_g^{\gamma}$**
- **Fits by Hudgins et al. published in 2003 remain the standard**

Direct-Bandgap Semiconductors

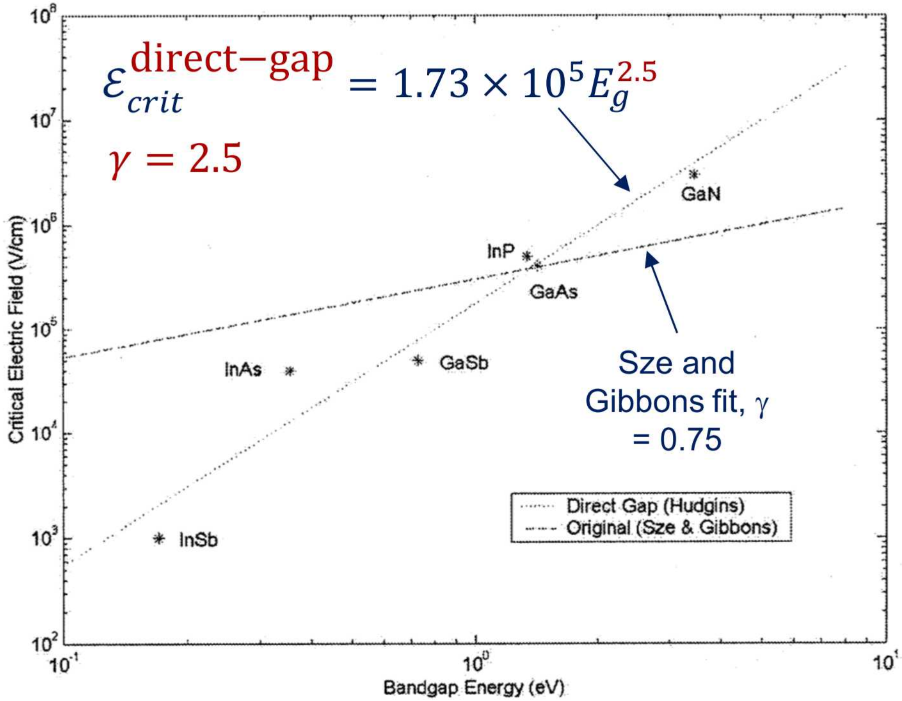

Indirect-Bandgap Semiconductors

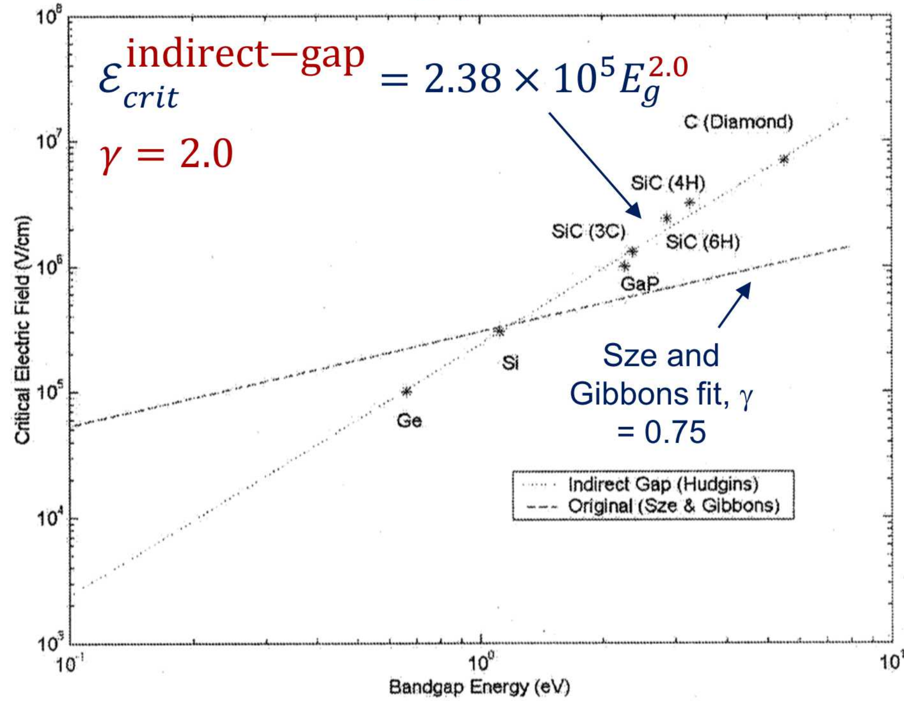

- **Empirical fits to data from the literature**
- **Not normalized to doping or device structure**

Normalization of Literature $\mathcal{E}_{crit}$ Values Results in Updated Power-Law

- **Normalized literature values to NPT structure with $N_D = 1\times10^{16}$ cm^{-3}**
- **Best-fit power-law slope gives $\mathcal{E}_{crit} \sim E_g^{\gamma}$ with $\gamma = 1.86$**

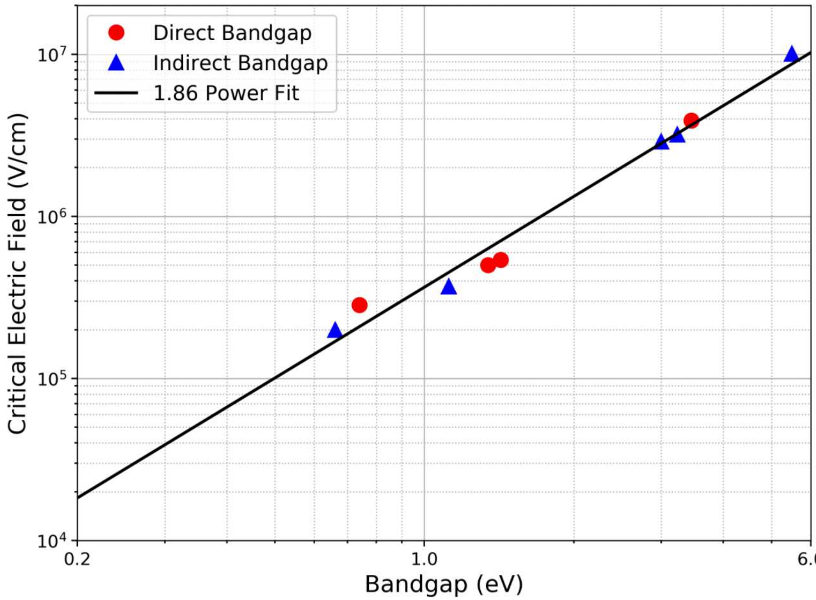

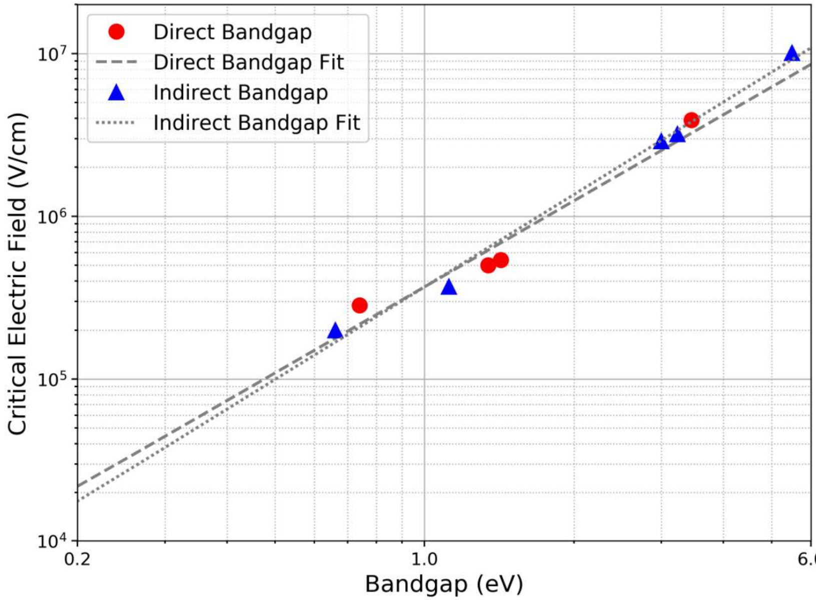

Semiconductor	Type	Bandgap (eV)	Normalized values
Ge	Indirect	0.661	2.0×10^5
$In_{0.53}Ga_{0.47}As$	Direct	0.74	2.8×10^5
Si	Indirect	1.12	3.7×10^5
InP	Direct	1.344	5.0×10^5
GaAs	Direct	1.424	5.4×10^5
6H-SiC	Indirect	3.0	2.9×10^6
4H-SiC	Indirect	3.23	3.2×10^6
GaN	Direct	3.45	3.9×10^6
C (diamond)	Indirect	5.5	1.0×10^7

Criticial Field Values	Slope	R^2
All	1.86	0.980
Direct Bandgap	1.76	0.947
Indirect Bandgap	1.89	0.992

No significant difference between direct- and indirect-bandgap materials

Comparison of Updated Power-Law Fit to Historical Fits

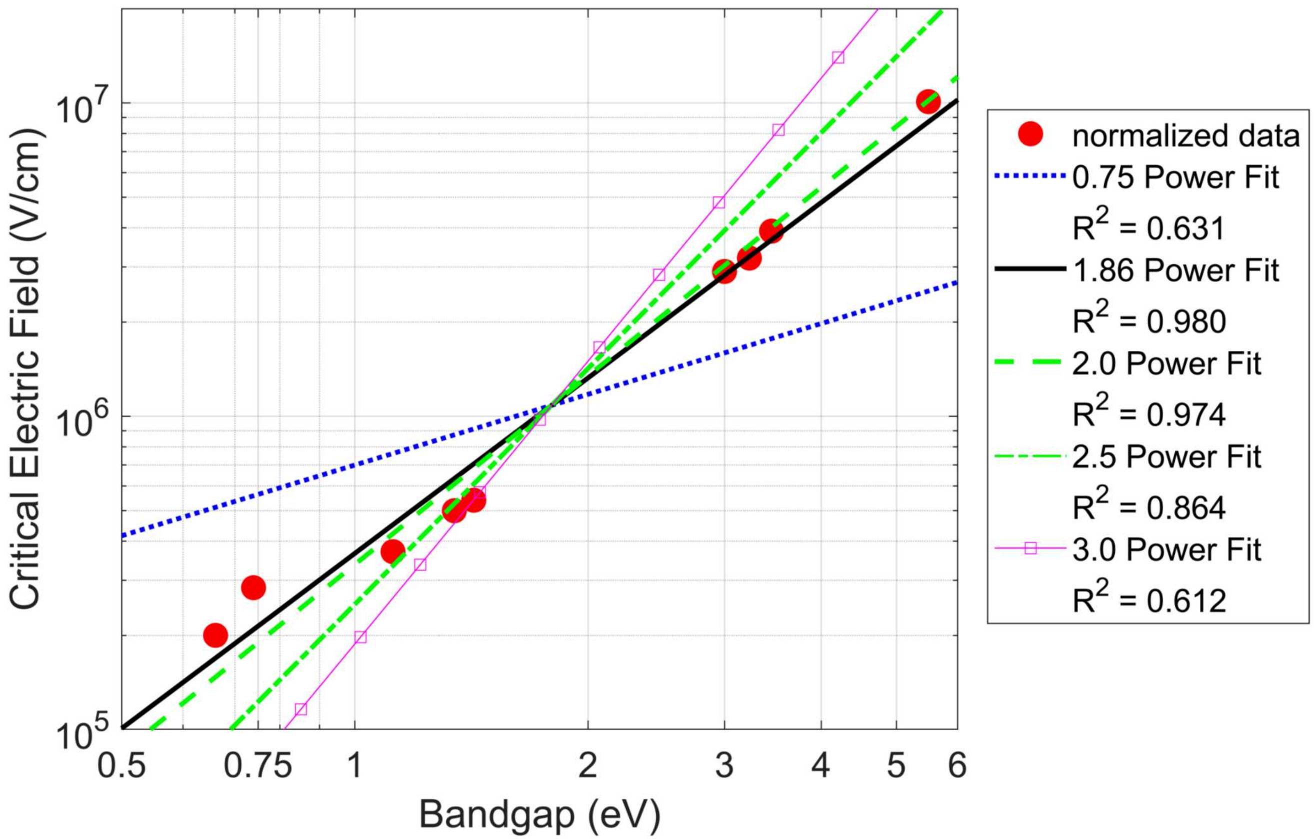

Sze & Gibbons

This work

Hudgins et al.

Hudgins et al.

Wang et al.

For normalized data, the proposed 1.86 power-law fit is better than most historical fits to date

Tradeoff Between $\mathcal{E}_{crit}$ and Mobility as Bandgap Increases

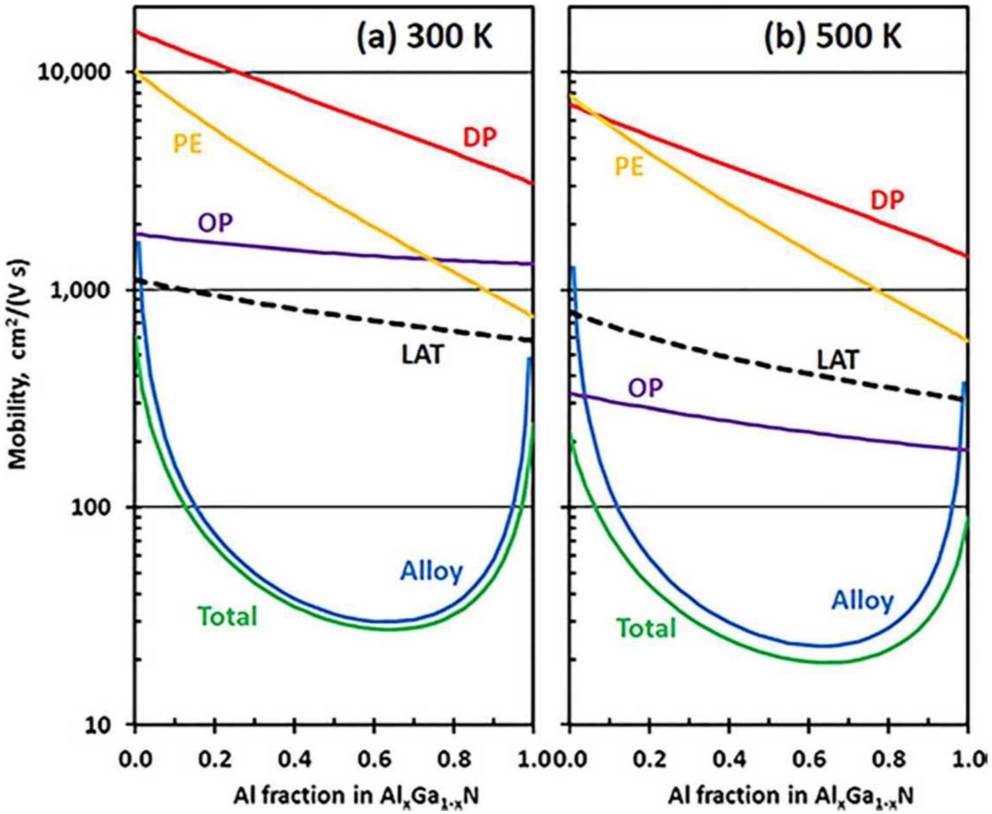

- Alloy scattering believed to dominate low-field transport in AlGaN
- Results in weak temperature dependence of mobility
- May be advantageous for high-temperature electronics

Unipolar FOM = $V_B^2/R_{on,sp} = \varepsilon\mu_n E_C^3/4$

M. E. Coltrin and R. J. Kaplar, J. Appl. Phys. 121, 055706 (2017)

Outline

- Motivation for UWBG Semiconductors
- **Vertical AlGaN PiN Diodes for Power Switching**
- Lateral AlGaN HEMTs for Power Switching
- Lateral AlGaN HEMTS for RF Applications

Power Electronics Volume and Weight Considerations

Passive elements and thermal management comprise the bulk of the volume and mass of a power converter

WBG/UWBG semiconductors enable higher switching frequency and reduction in size of passive elements and thermal management

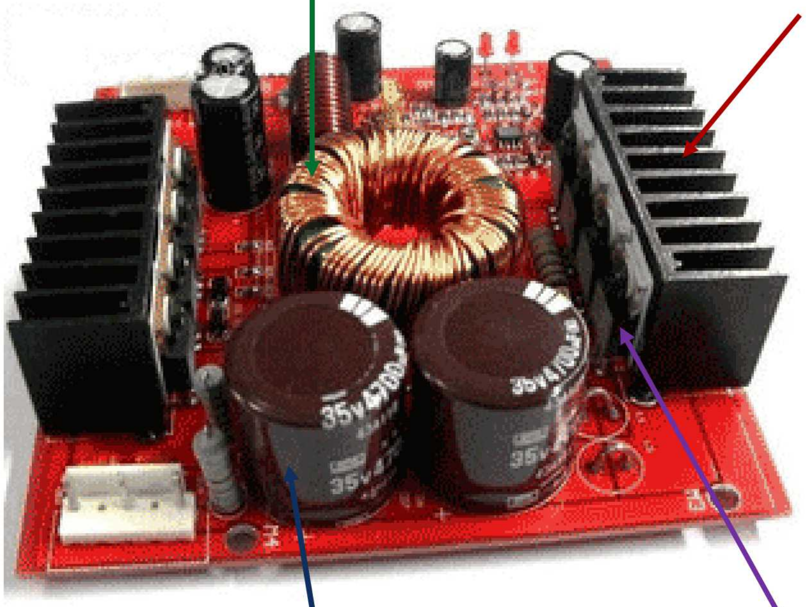

WBGs and UWBGs Enable Dramatic Reduction in Power Converter Volume

SiC converter is 10% the volume and weight of Si for equivalent capability (10 kV, 100 A)

UWBG materials and devices may enable *additional reduction* in power converter size and weight!

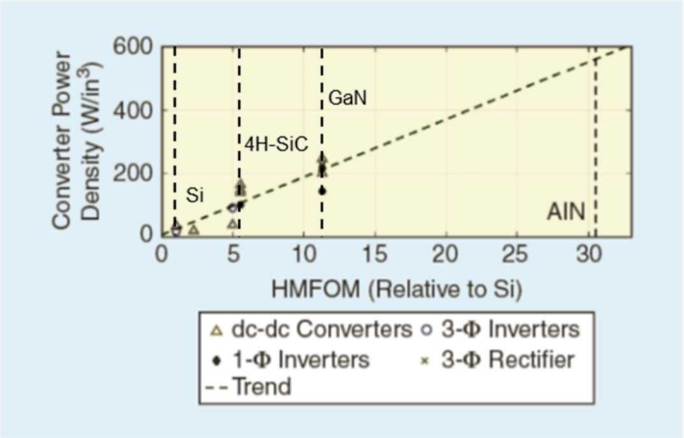

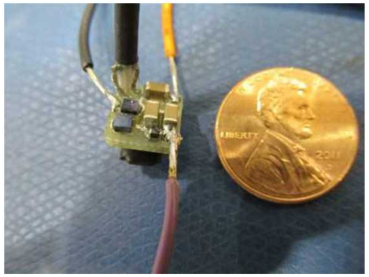

SNL "Coin Converter"
90 V, 90 mA → 215 W/in^3

R. J. Kaplar, J. C. Neely, et al., *IEEE Power Electronics Magazine (March 2017)*

Literature Data on Vertical AlGaN PiN Diodes

$Al_xGa_{1-x}N$ *vertical* PiN diode ($0 < x_{Al} < 0.57$)

- **Drift Layer: ~ 0.2 μm, n ~ 2×10^{16} cm^{-3}**
- **n-SiC substrates, $R_{on,sp}$ = 1.45 mΩ-cm^2 (x_{Al} = 0.22)**

Drift region

Vertical injection

Conducting SiC substrate

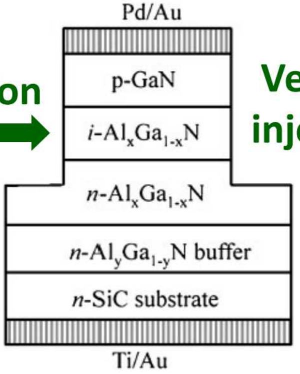

Reverse breakdown < 200 V

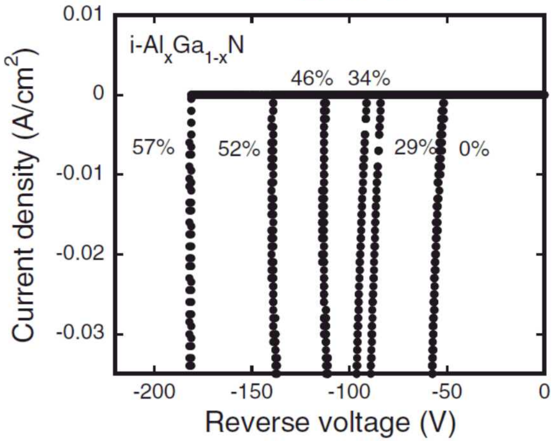

Effective E_C ~ 8 MV/cm (2x GaN)

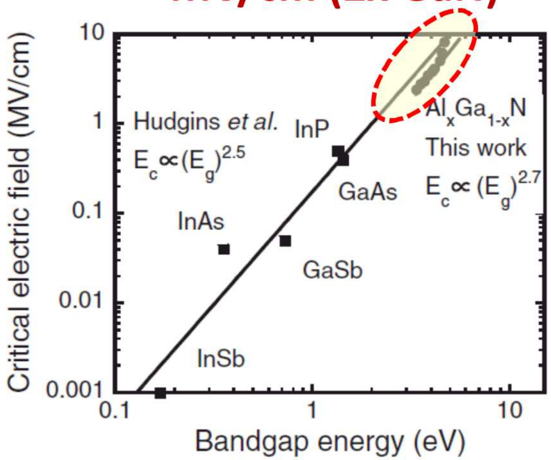

Higher forward turn-on for increasing Al %

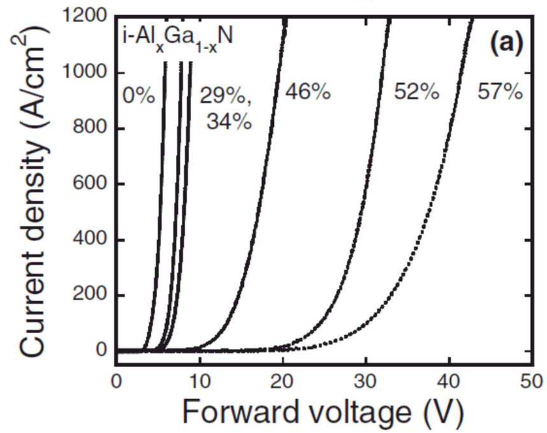

- ➢ **Breakdown voltage increases with larger bandgap**
- ➢ **Effective critical electric field scales as $E_G^{2.7}$**

Nishikawa et al. JJAP 46 (4B), 2316 (2007)

kV-Class Quasi-Vertical $Al_{0.3}Ga_{0.7}N$ PiN Diode

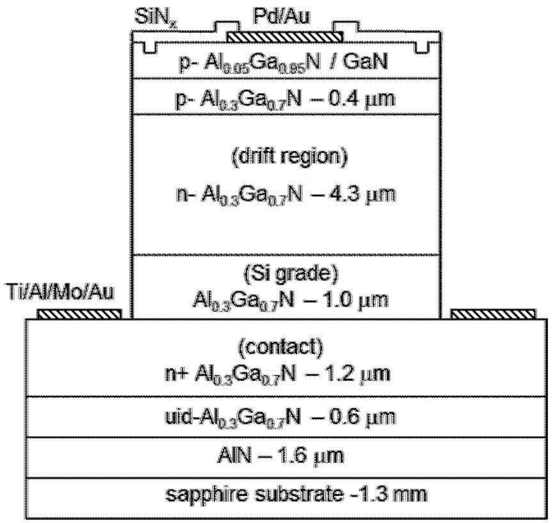

- Drift region doping mid-10^{16} cm^{-3} *n*-type
- Record $V_B^2/R_{on,sp}$ = 150 MW/cm^2, *>20x better than any previously published result*
- Drift region thickness = 4.3 μm, likewise >20x greater than previously published results
- Current density up to 3.5 kA/cm^2 measured

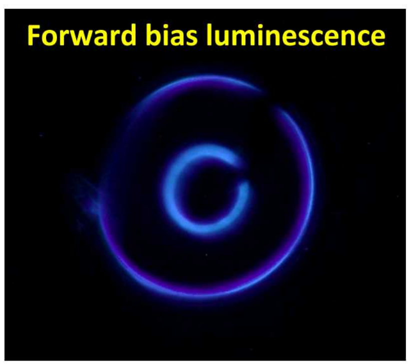

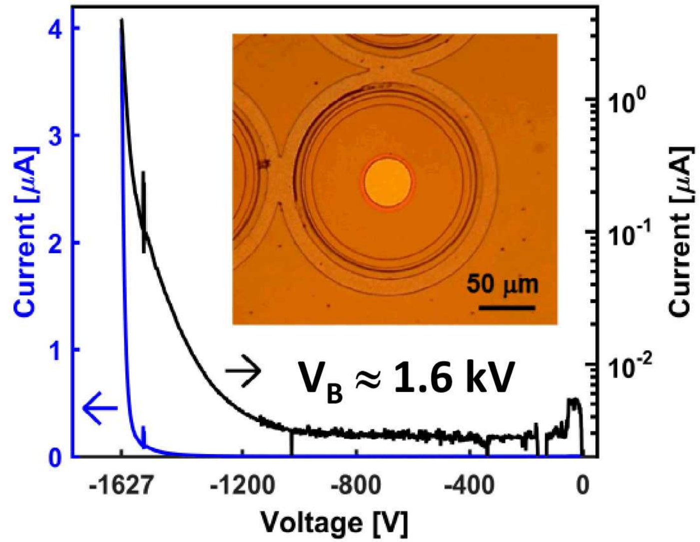

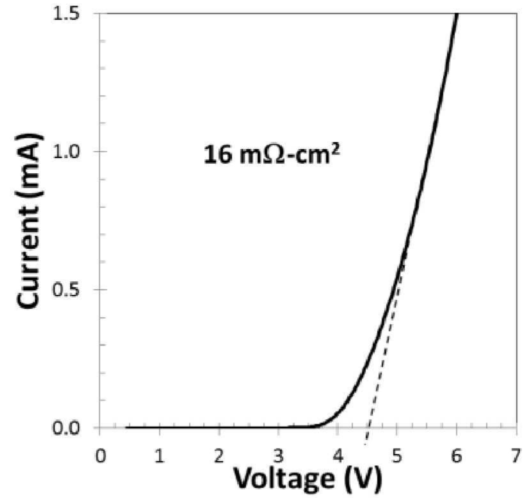

A. Allerman et al., Elec. Lett. 52(15), 1319 (2016)

On-resistance likely limited by quasi-vertical design

Critical Electric Field Scaling and Thicker Drift Regions for Higher V_B

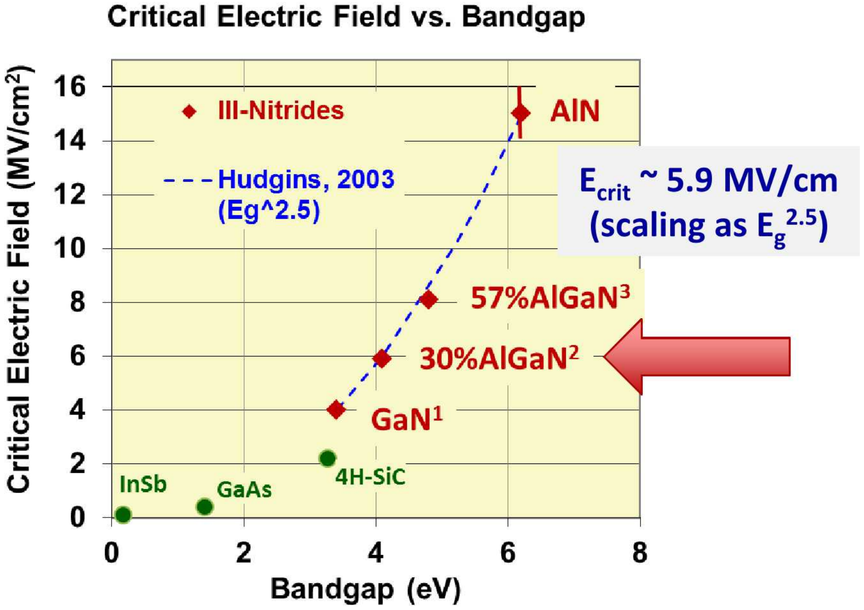

- **4.3 μm $Al_{0.3}Ga_{0.7}N$ drift region is punched-through at breakdown**
- **Punch-through analysis indicates effective E_C = 5.9 MV/cm, consistent with E_C~$E_G^{2.5}$ scaling**

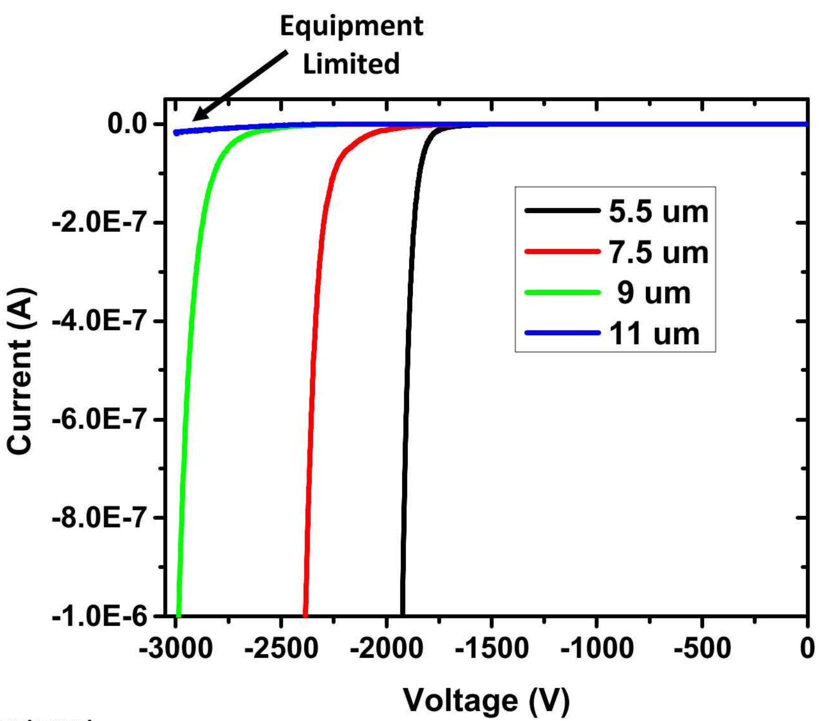

Devices grown using thicker drift regions show higher breakdown voltage

1 – Armstrong EL 2016; 2 – Allerman EL 2016; 3 – Nishikawa et al. JJAP 46 (4B), 2316 (2007)

Comparison of Breakdown Voltages Reported for III-N PiN Diodes

GaN diode (Vertical)

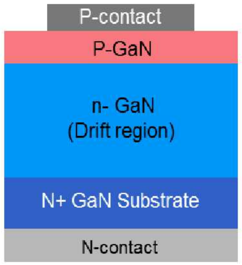

AlGaN di (Quasi-ver

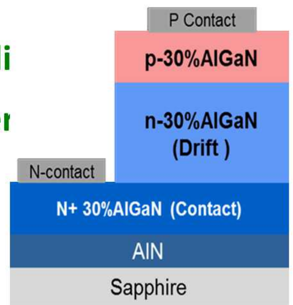

Breakdown (kV)	No (cm-3)	Drift (um)	Material	Group	Ref
4.7 / 5.0	2-16e15	33	GaN	Hosei Univ.	EDL 36 p1180 (2015) / Jpn J Appl. P. 57 (2018)
4.0	2-5e15	40	GaN	Avogy	EDL 36 p1073 (2015)
3.9	3e15	30	GaN	Sandia	EL 52 p1170 (2016)
3.7	5e15	>30	GaN	Avogy	EDL 35 p247 (2014)
3.5	1-12e15	32	GaN	Hosei Univ.	IEDM15-237 (2015)
>3	0.8-3e16	11	30%-AGaN	Sandia	This work
3.0	0.8-3e16	9	30%-AGaN	Sandia	This work
3.0	1-10e15	20	GaN	Hitachi	Jpn J Appl Phys 52 p028007 (2013)

Advantages of Ultra-Wide-Bandgap AlGaN

	GaN	$Al_{0.3}Ga_{0.7}N$	
N_o (cm^{-3})	low 10^{15}	low 10^{16}	← Larger E_C & E_G
Drift (μm)	20-30	~10	
TDD (cm^{-2})	≤ 10^6	low 10^9	← Impact?

Outline

- Motivation for UWBG Semiconductors
- Vertical AlGaN PiN Diodes for Power Switching
- **Lateral AlGaN HEMTs for Power Switching**
- Lateral AlGaN HEMTS for RF Applications

Lateral Power Device Figure of Merit

- **Not as widely known as the unipolar FOM**
- **Unipolar (vertical) FOM is often incorrectly used for lateral devices**

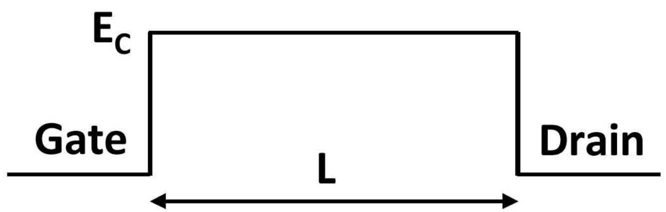

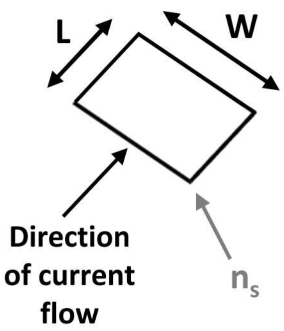

$$V_B = E_C L$$

$$R_{on} = \frac{L}{Wq\mu_{ch}n_s}$$

$$R_{on,sp} = R_{on}WL = \frac{L^2}{q\mu_{ch}n_s}$$

$$FOM = \frac{V_B^2}{R_{on,sp}} = q\mu_{ch}n_s E_C^2$$

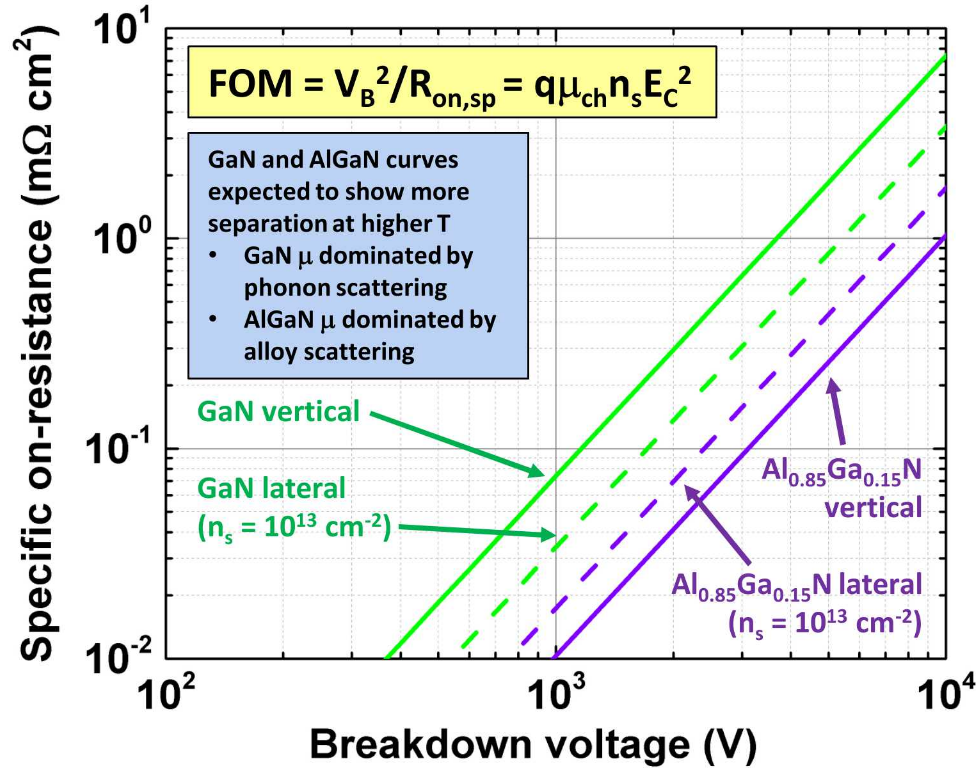

- **Proportional to E_C^2 rather than E_C^3, but high n_s can result in high FOM**

$Al_{0.85}Ga_{0.15}N/Al_{0.70}Ga_{0.30}N$ UWBG HEMT Structure

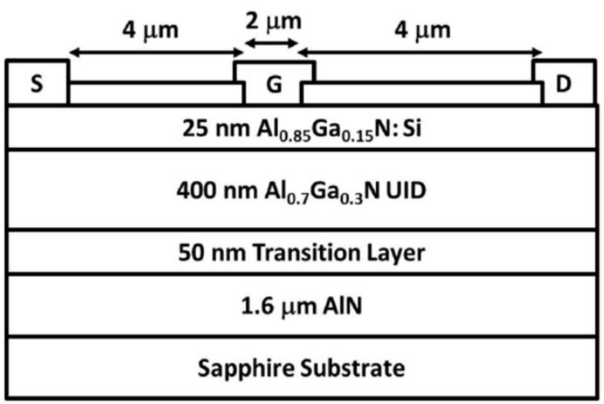

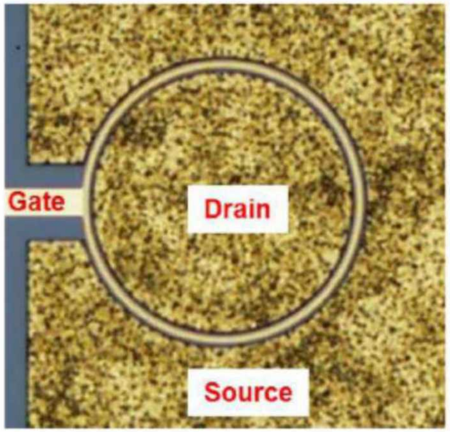

CV Characterization

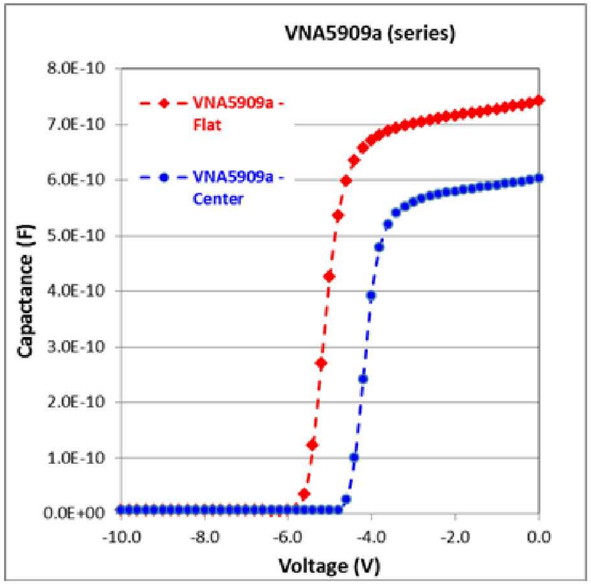

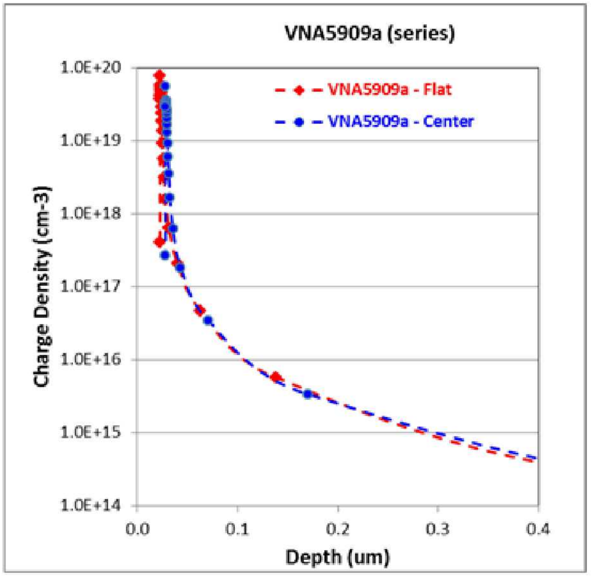

Planar source and drain contacts

- **Sheet resistance: 2200 $\Omega/\square$**
- **Pinch-off voltage: -4.5 V (center)**
- **Sheet charge density: 6×10^{12} cm^{-2}**
- **Inferred mobility: 250 cm^2/Vs**

A. G. Baca et al., ECS J. Solid-State Sci. Tech. 6 (12), Q161 (2017)

Electrical Characteristics of $Al_{0.85}Ga_{0.70}N/Al_{0.70}Ga_{0.30}N$ HEMT

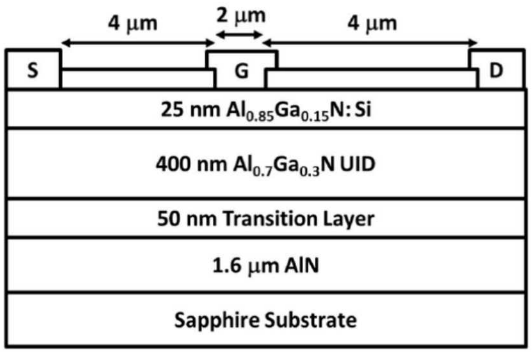

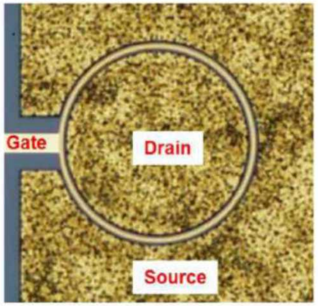

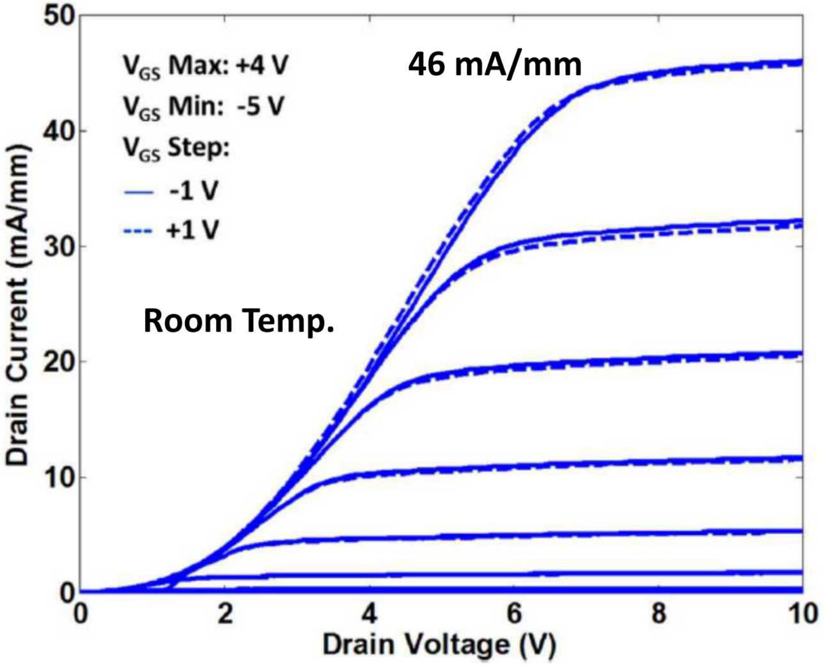

- **Current density**
  - **Current density of 46 mA/mm (good, but < 2x expected based on channel properties)**
  - **Due to quasi-rectifying behavior in source and drain contacts**
- **Sub-threshold slope ~ 75 mV/decade**

A. G. Baca et al., ECS J. Solid-State Sci. Tech. 6 (12), Q161 (2017)

Operation of $Al_{0.85}Ga_{0.70}N/Al_{0.70}Ga_{0.30}N$ HEMT Over Wide Temperature Range

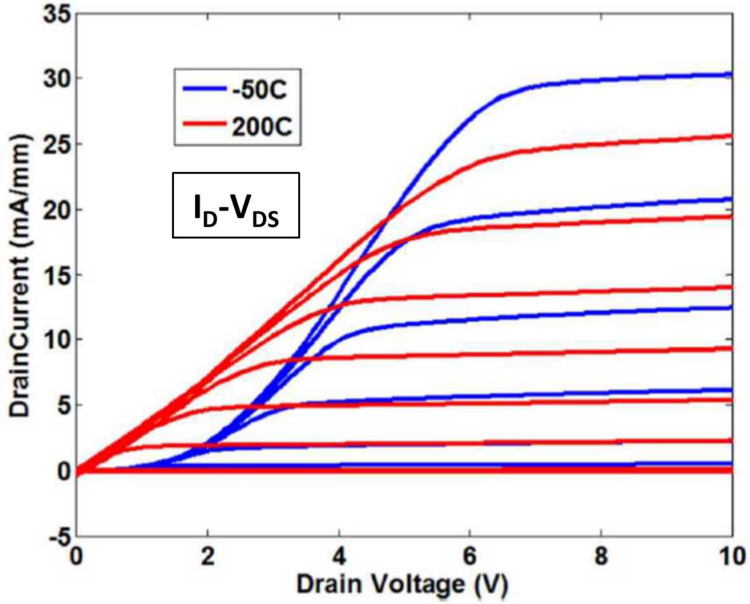

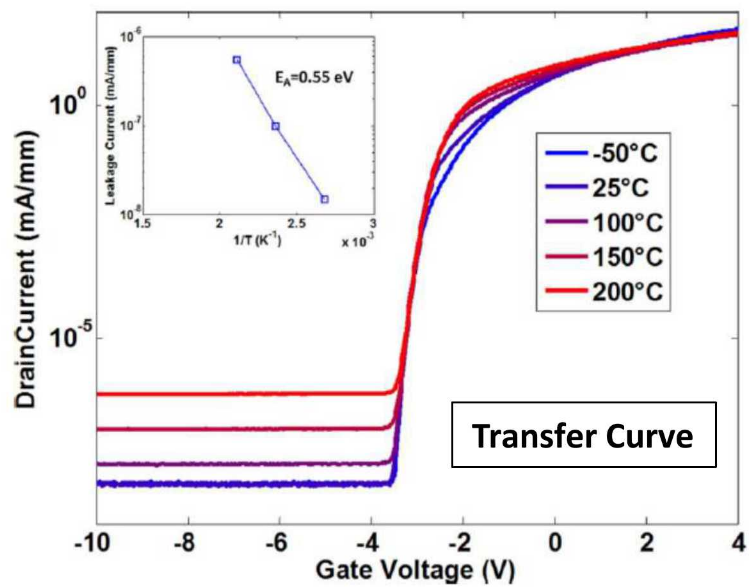

- **Relatively weak dependence on temperature**
- **Likely due to insensitivity of channel mobility to temperature**
- **Ohmic contacts improve at high temperature**

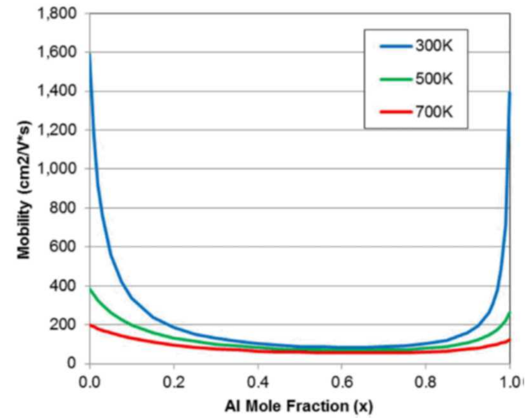

Channel mobility vs. temperature for 2DEG in AlGaN/AlGaN heterostructure

A. G. Baca et al., ECS J. Solid-State Sci. Tech. 6 (12), Q161 (2017); M. E. Coltrin, A. G. Baca, and R. J. Kaplar, ECS J. Solid-State Sci. Tech. 6 (11), S3114 (2017)

Breakdown Voltage of $Al_{0.85}Ga_{0.70}N/Al_{0.70}Ga_{0.30}N$ HEMT

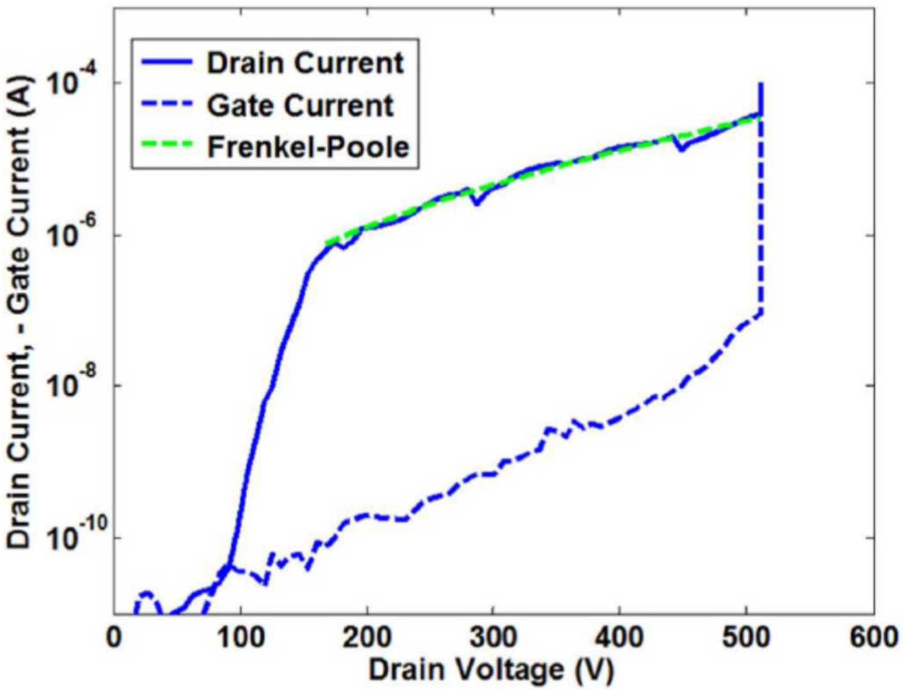

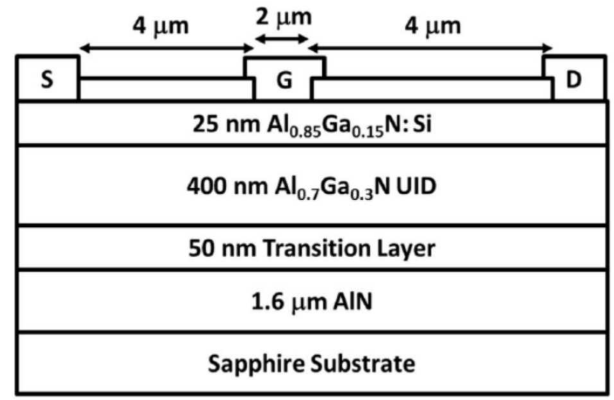

- **Field plate with SiN dielectric**
- **Misalignment with a circular gate leads to L_{GD} (actual) < L_{GD} (drawn)**
- **V_{br} = 511 V**
  - **L_{GD} = 1.6-5.4 μm (single device with misalignment)**
- **Breakdown field = 95-320 V/μm (≈ 1.0-3.2 MV/cm)**
  - **Exceeds previous generation device (81 V/μm)**
  - **GaN HEMT typical breakdown field ≈ 100 V/μm**

A. G. Baca et al., ECS J. Solid-State Sci. Tech. 6 (12), Q161 (2017)

Ohmic Contact Development for Al-Rich AlGaN HEMTs

$Al_{0.45}Ga_{0.55}N/Al_{0.30}Ga_{0.70}N$

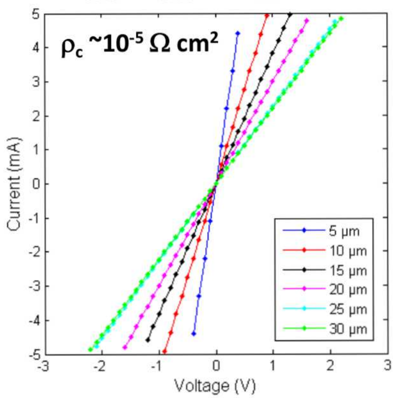

$Al_{0.85}Ga_{0.15}N/Al_{0.70}Ga_{0.30}N$

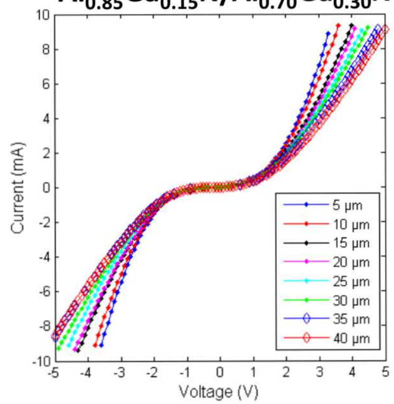

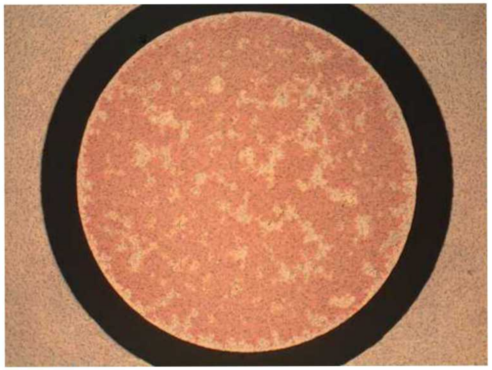

Au 50 nm
Ni 15 nm
Al 100 nm
Ti 25 nm
AlGaN/Substrate

900°C anneal

50 nm $Al_{0.45}Ga_{0.55}N$
4.15 mm $Al_{0.3}Ga_{0.7}N$
1.6 mm AlN
Sapphire Substrate

25 nm $Al_{0.85}Ga_{0.15}N$
400 nm $Al_{0.7}Ga_{0.3}N$
Graded Layer 50 nm
2.9 mm AlN
Sapphire Substrate

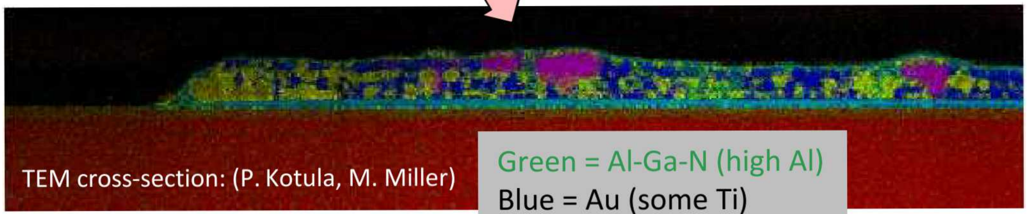

B. A. Klein et al., ECS J. Solid-State Sci. Tech. 6 (11), S3067 (2017)

Graded heterostructure approach

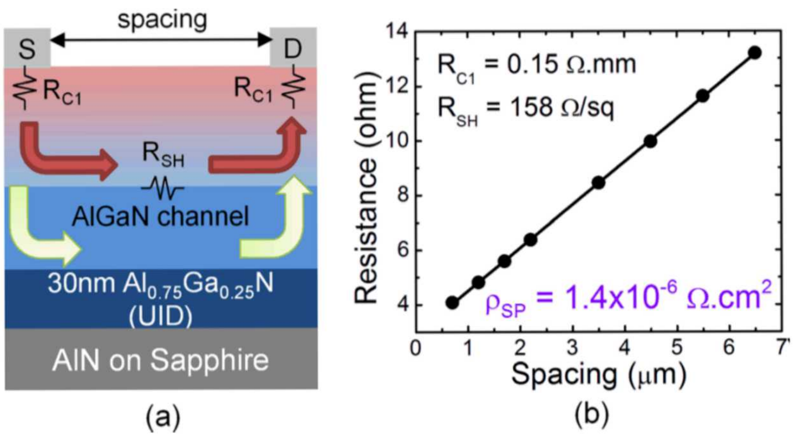

S. Bajaj et al., Appl. Phys. Lett. 133508 (2016)

Outline

- Motivation for UWBG Semiconductors
- Vertical AlGaN PiN Diodes for Power Switching
- Lateral AlGaN HEMTs for Power Switching
- **Lateral AlGaN HEMTS for RF Applications**

Radio-Frequency Applications

- More powerful radar has longer range
- Beam can be focused down to interact with incoming target’s guidance electronics
- Can be used in smaller directed energy applications to heat opponent's skin
- Can use as a high power microwave system to locally affect operation of electronics

K. Jones, ARL

Advantages of UWBGs for Radio-Frequency Devices

Critical electric field

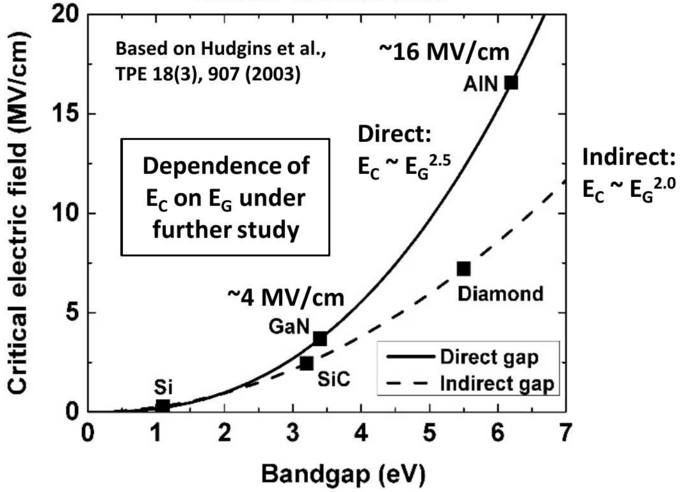

Saturation velocity

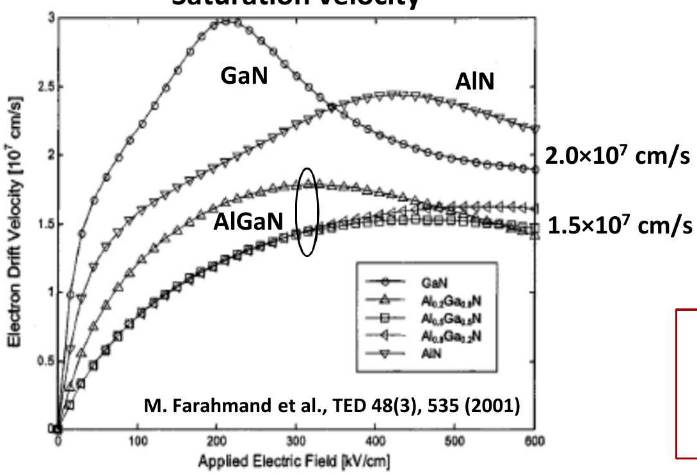

Johnson FOM: $V_B f_T = E_C v_{sat}/2\pi$

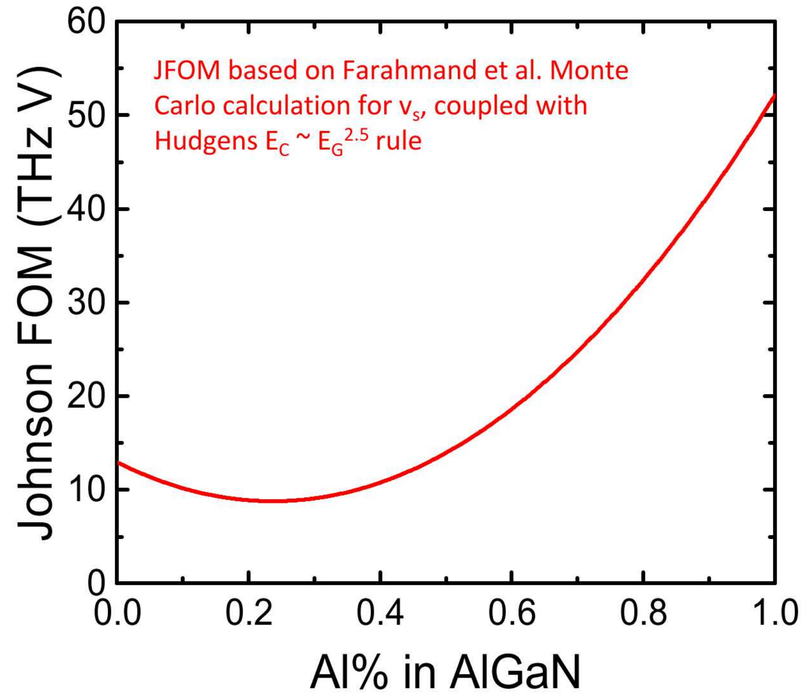

Al-rich AlGaN yields better JFOM than GaN due to higher E_C and comparable v_{sat}

Predicted 8× RF Power Density Increase for Al-Rich HEMTs Compared to GaN-Channel HEMTs

- Maximum power density $P_{max} = J_{max}V_{max}/8$ with $J_{max} = qv_{sat}n_s$

- Three factors plausibly lead to 8× power density for Al-rich AlGaN HEMTs compared to GaN-channel HEMTs **(GaN: ~4 W/mm → AlGaN: >30 W/mm)**
  - 4× greater breakdown voltage for same dimensions (V_{max})
  - 2× sheet carrier density (J_{max})
  - Parity in electron saturation velocity (J_{max})

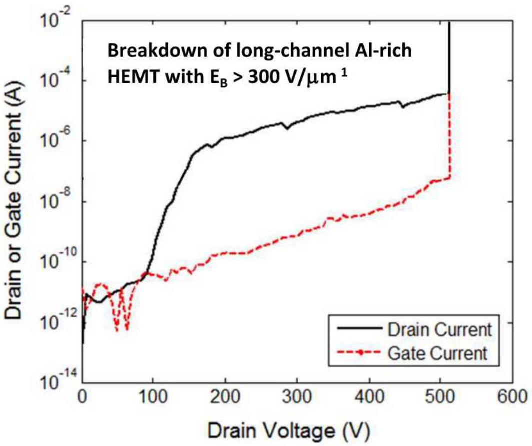

- Breakdown electric field is typically ~4× lower than theoretical
  - ~400 V/µm expected for Al-rich $Al_xGa_{1-x}N$ with x close to 1
  - >300 V/µm observed experimentally for $x = 0.7$
  - Compared to ~100 V/µm for GaN

- 2DEG sheet density $n_s > 2\times10^{13}$ cm^{-2}
  - Potentially higher bandgap offset
  - Larger polarization charge for higher x
  - Potential to grow thick, compressively strained barrier layer on AlN substrates

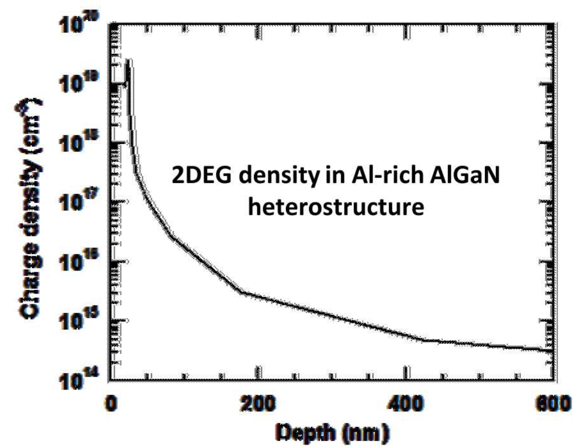

- v_s ~ 4×10^6 cm/s measured in $Al_{0.7}Ga_{0.3}N$ (~35% that of GaN) [2]

1 – A. G. Baca et al., ECS J. Solid-State Sci. Tech. 6 (12), Q161 (2017)
2 – B. A. Klein et al., J. Elec. Mat. DOI 10.1007/s11664-019-07421-1 (2019)

$Al_{0.85}Ga_{0.15}N/Al_{0.70}Ga_{0.30}N$ HEMT with 80 nm Gate

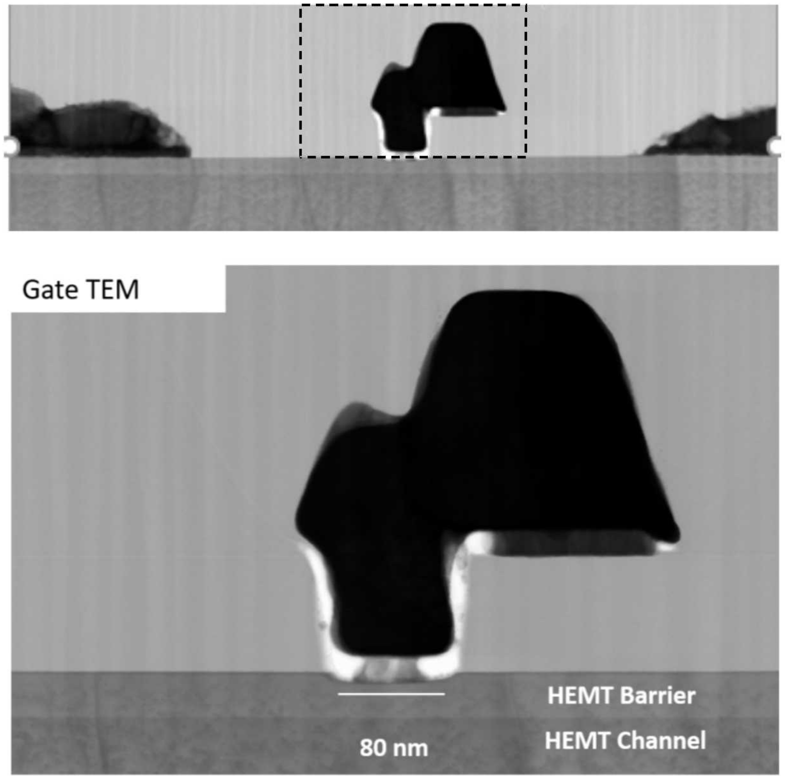

- 30 nm thick $Al_{0.85}Ga_{0.15}N$ barrier and 400 nm thick $Al_{0.70}Ga_{0.30}N$ channel + buffer
  - MOCVD growth on sapphire substrate
  - AlN nucleation + graded transition layers
- Barrier doped with 3.5×18 cm^{-3} Si
- 2DEG resistivity ~2200 Ω/sq → μ_{ch} ≈ 390 cm^2/Vs, n_s ≈ 7.2×10^{12} cm^{-2}
- Nb/Ti/Al/Mo/Au source and drain contacts
- Ni/Au gate with field plate on SiN_x
- Maximum DC current density ≈ 160 mA/mm at V_{ds} = 10 V, V_{gs} = 10 V

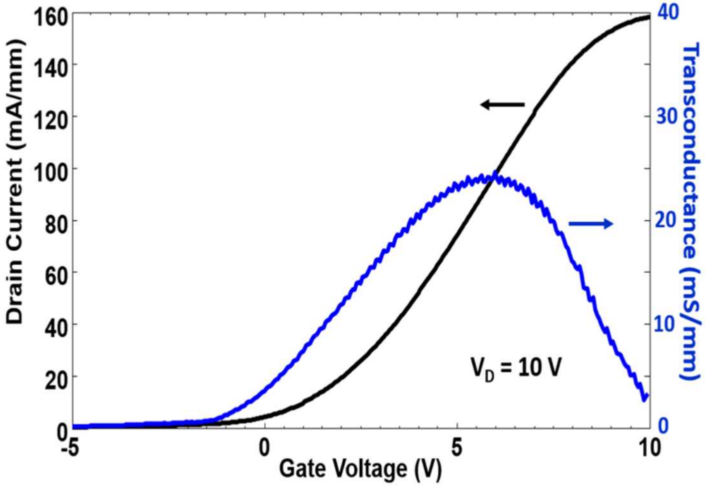

A. G. Baca et al., EDL 40(1), 17 (2019)

RF Characteristics of $Al_{0.85}Ga_{0.15}N/Al_{0.70}Ga_{0.30}N$ HEMT

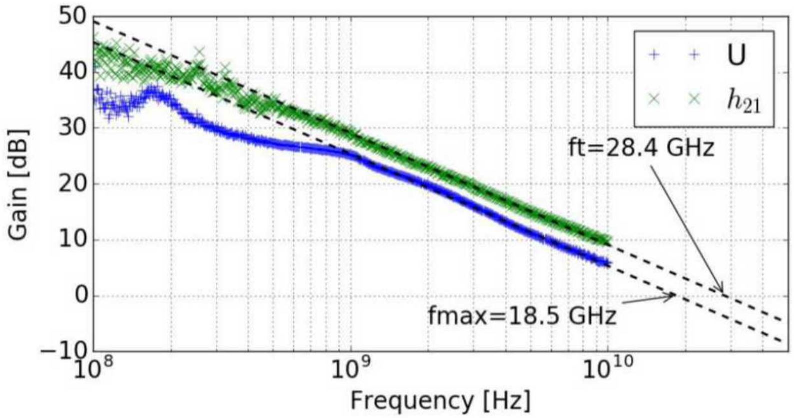

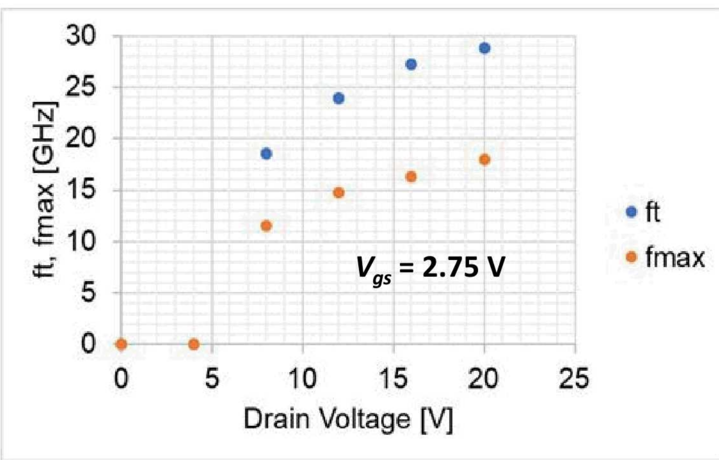

- **f_T and f_{max} extracted from s-parameter measurements at V_{ds} = 20 V, V_{gs} = 2.75 V**
  - **f_T ≈ 28.4 GHz, f_{max} ≈ 18.5 GHz**
  - **Reversal in order may be due to large gate resistance and/or channel conductance**
- **Power sweep at 3 GHz, V_{ds} = 20 V, V_{gs} = 2.75 V**
  - **Output power ≈ 0.38 W/mm (15.8 dBm) at maximum PAE of 11%**
  - **Maximum power gain G_P ≈ 7.3 dB**
- **Well below theoretical and simulated values**
  - **Comparable to other emerging UWBG RF technologies**
  - **Better Ohmic contacts may help**

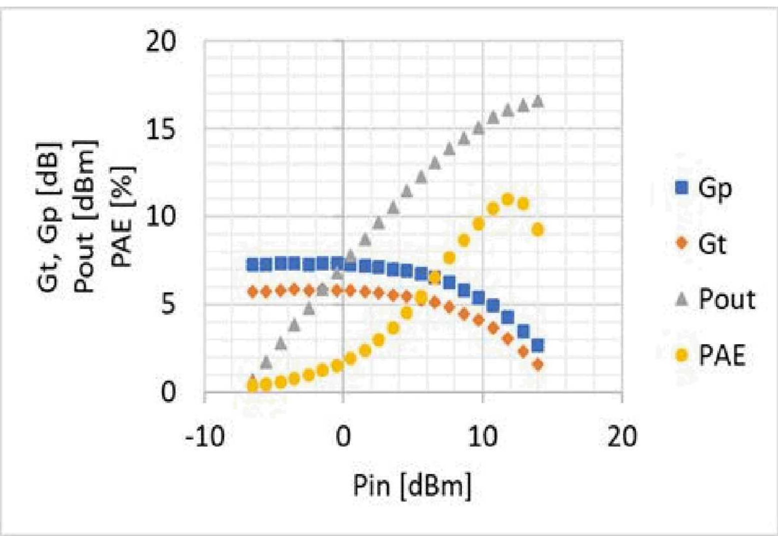

A. G. Baca et al., EDL 40(1), 17 (2019)

Summary

- UWBGs, including Al-rich AlGaN, represent the next generation in semiconductor physics
- Advantages are due to expected superior material properties such as high critical electric field for avalanche breakdown
- Confers advantages to several applications:
  - Power switching: Lower system size and weight
  - RF applications: Greater power density
  - Insensitive to temperature variation
- Several Al-rich AlGaN device types demonstrated:
  - Vertical PiN diodes
  - Lateral power-switching HEMTs (long-channel)
  - Lateral RF HEMTs (short-channel)